ACS Catalysis

Research Article

pubs.acs.org/acscatalysis

Screening of Catalysts for Hydrodeoxygenation of Phenol as a Model Compound for Bio-oil

Peter M. Mortensen,[†] Jan-Dierk Grunwaldt,[‡] Peter A. Jensen,[†] and Anker D. Jensen*[,†]

[†]Department of Chemical and Biochemical Engineering, Technical University of Denmark, Søltofts Plads, Building 229, DK-2800 Lyngby, Denmark

[‡]Institute for Chemical Technology and Polymer Chemistry, Karlsruhe Institute of Technology (KIT), Engesserstrasse 20, D-79131 Karlsruhe, Germany

Supporting Information

ABSTRACT: Four groups of catalysts have been tested for hydrodeoxygenation (HDO) of phenol as a model compound of bio-oil, including oxide catalysts, methanol synthesis catalysts, reduced noble metal catalysts, and reduced non-noble metal catalysts. In total, 23 different catalysts were tested at 100 bar H_2 and 275 °C in a batch reactor. The experiments showed that none of the tested oxides or methanol synthesis catalysts had any significant activity for phenol HDO under the given conditions, which were linked to their inability to hydrogenate the aromatic ring of phenol. HDO of phenol over reduced metal catalysts could effectively be described by a kinetic model involving a two-step reaction in which phenol initially was hydrogenated to cyclohexanol and then subsequently deoxygenated to cyclohexane. Among reduced noble metal catalysts, ruthenium, palladium, and platinum were all found to be active, with activity decreasing in that order. Nickel was the only active non-noble metal catalyst. For nickel, the effect of support was also investigated and ZrO_2 was found to perform best. Pt/C, Ni/CeO_2, and Ni/CeO_2-ZrO_2 were the most active catalysts for the initial hydrogenation of phenol to cyclohexanol but were not very active for the subsequent deoxygenation step. Overall, the order of activity of the best performing HDO catalysts was as follows: Ni/ZrO_2 > Ni-V_2O_5/ZrO_2 > Ni-V_2O_5/SiO_2 > Ru/C > Ni/Al_2O_3 > Ni/SiO_2 ≫ Pd/C > Pt/C. The choice of support influenced the activity significantly. Nickel was found to be practically inactive for HDO of phenol on a carbon support but more active than the carbon-supported noble metal catalysts when supported on ZrO_2. This observation indicates that the nickel-based catalysts require a metal oxide as a carrier on which the activation of the phenol for the hydrogenation can take place through heterolytic dissociation of the O−H bond to facilitate the reaction.

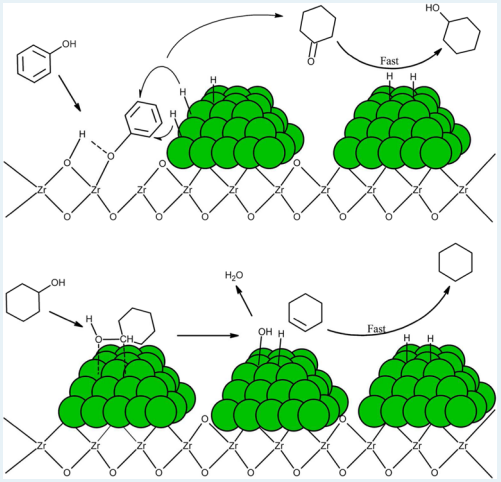

KEYWORDS: *bio-oil, catalyst screening, hydrodeoxygenation, noble metals, phenol, oxides, reduced metals*

1. INTRODUCTION

A prospective route for production of biofuels is the conversion of biomass into bio-oil through flash pyrolysis followed by upgrading via hydrodeoxygenation (HDO).[1] Flash pyrolysis is advantageous in making a locally produced liquid that minimizes transportation costs to larger biorefineries.[2−4] However, bio-oil is a viscous, polar, and acidic liquid with a low heating value, making it, in most cases, unsuitable as an engine fuel directly. These unfavorable characteristics are all associated with high levels of water (10−30 wt %) and oxygen-containing organic compounds (30−40 wt % oxygen) in the oil.[5]

In HDO, bio-oil is treated with hydrogen at a pressure of up to 200 bar and temperatures in the range from 200 to 400 °C. This converts the oxy compounds to a hydrocarbon product that is separated from the water and ultimately gives a product equivalent to crude oil. The reaction can be generally written as (normalized to feed carbon)[1]

$$CH_{1.4}O_{0.4} + 0.7H_2 \rightarrow \text{“}CH_2\text{”} + 0.4H_2O \quad (1)$$

where “CH_2” represents an unspecified hydrocarbon as a product.

One of the major challenges with this concept is to find a catalyst with a high activity for the deoxygenation reaction and at the same time obtain a sufficient lifetime, as deposition of carbonaceous species has proven to be a severe problem.[1,6] Preferably, HDO catalysts should be relatively inexpensive and function at low temperatures (<300 °C) and low pressures (<100 bar). In particular, low temperatures are desirable to prevent coking,[1,7] and therefore, focus has in the current screening study been on catalysts operating at 275 °C. Four categories of catalysts were tested as catalysts for HDO of

Received: April 9, 2013
Revised: June 26, 2013
Published: July 1, 2013

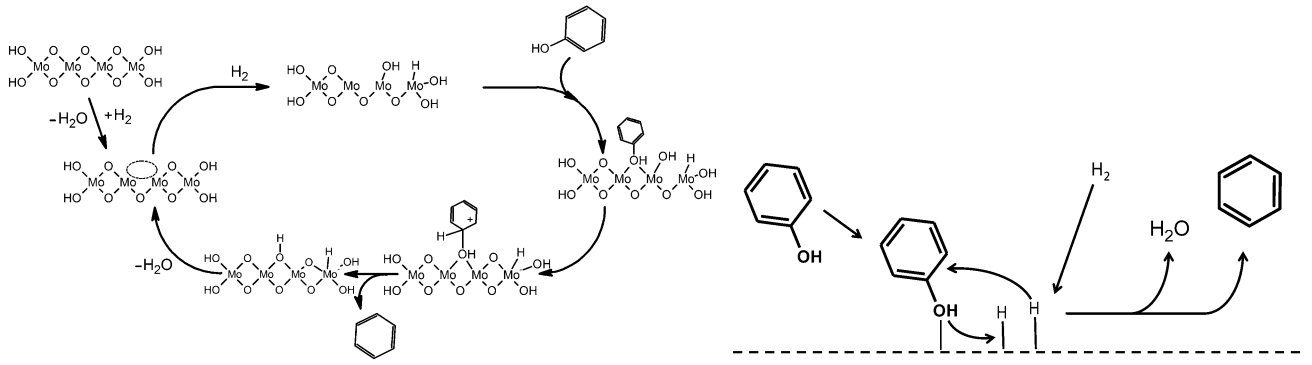

(a) Oxide catalysts reaction mechanism (b) Reduced metal catalysts reaction mechanism

Figure 1. Proposed reaction mechanisms of (a) oxide catalysts[1,10] and (b) reduced metal catalysts.[11,12]

Table 1. Summary of Catalyst and Support Properties, i.e., the Theoretical Loading of the Active Component, the Particle Size of the Support (Sieve Fraction), the Specific Surface Area, and Reduction Conditions for the Tested Catalysts

catalyst/support	loading (wt %)	particle size (μm)	surface area (m^2/g)	reduction T (°C)/t (h)
carbon	–	–	1100	–
SiO_2	–	–	250	–
ZrO_2	–	–	160	–
CeO_2	–	–	140	–
CeO_2-ZrO_2	–	–	140	–
$MgAl_2O_4$	–	–	90	–
Al_2O_3	–	–	150	–
MnO/C	15	710–1400	680	none
WO_3/C	15	710–1400	790	none
MoO_3/C	15	710–1400	660	none
V_2O_5/C	15	710–1400	310	none
NiO-MoO_3/Al_2O_3[a]	–	300–600	–	none
CoO-MoO_3/Al_2O_3[a]	–	300–600	–	none
Cu/ZnO/Al_2O_3	45% Cu/5% Zn	≈900	60	300/7
NiCu/SiO_2	10% Ni/10% Cu	≈900	180	350/19
Cu/SiO_2	15	300–600	170	380/19
Ru/C	5	≈15	1160	400/2
Pd/C	5	≈15	1100	400/2
Pt/C	5	≈15	1140	400/2
Co/SiO_2	5	300–600	210	550/2
Fe/SiO_2	5	300–600	200	550/2
Ni/SiO_2	5	63–125	210	400/2
Ni/Al_2O_3	5	63–125	140	550/2
Ni/CeO_2	5	63–125	130	400/2
Ni/ZrO_2	5	63–125	130	550/2
Ni/CeO_2-ZrO_2	5	63–125	120	550/2
Ni/$MgAl_2O_4$	5	63–125	80	550/2
Ni/C	5	63–125	1020	550/2
Ni-V_2O_5/SiO_2	5% Ni/5% V	300–600	210	550/2
Ni-V_2O_5/ZrO_2	5% Ni/5% V	300–600	120	550/2

[a]Commercial catalyst by Haldor Topsøe A/S without detailed characterization data.

phenol: (1) oxide catalysts, (2) methanol synthesis catalysts, (3) reduced noble metal catalysts, and (4) reduced non-noble metal catalysts. Phenol was chosen as a model compound of bio-oil, as phenols have been identified among the most persistent,[8] yet fairly abundant,[9] compounds in bio-oil.

Oxide catalysts have been proposed to catalyze the reaction through roughly three steps as shown in Figure 1a: chemisorption via the oxygen atom on a coordinatively unsaturated metal site, donation of a proton from a hydroxyl group, and desorption.[1,10] In this mechanism, the generation of vacancy sites (the dotted circle in the figure) is responsible for the activation of both the oxy compound and hydrogen on the catalytic surface.[1,10]

Methanol synthesis catalysts have proven to be able to activate CO/CO_2 through the oxygen.[13−16] Thus, these catalysts could potentially activate oxy compounds through their oxygen group and in this way permit reaction.

Figure 1b shows the key concepts of the reaction mechanism for reduced metal catalysts.[1] The reaction is initiated by adsorption of the oxy compound on the catalyst surface.

dx.doi.org/10.1021/cs400266e | ACS Catal. 2013, 3, 1774−1785

Adsorbed hydrogen on the active metal clusters reacts with the oxy compound to facilitate the deoxygenation. This is followed by desorption of the final product. The oxy compound adsorption step can take place either on the support or directly on the active metal, depending on which type of metal is used. Specifically, noble metals have been shown to be capable of activating the oxy compound on the metal sites.[12,17] For non-noble metals, the activation is thought to occur through an oxygen vacancy site in the support metal oxide,[11,18] similar to the activation step for the oxide catalysts shown in Figure 1a. Hence, these four different classes of catalysts were screened in this work.

2. EXPERIMENTAL SECTION

2.1. Catalyst Synthesis. MnO/C, WO_3/C, MoO_3/C, V_2O_5/C, Cu/SiO_2, NiCu/SiO_2, Co/SiO_2, Fe/SiO_2, Ni-based catalysts, and Ni-V-based catalysts were all prepared by incipient wetness impregnation of the corresponding supports. An overview of the applied catalysts is given in Table 1. The precursors for the active materials were $Mn(C_2H_3O_2)_2{\cdot}4H_2O$ (Sigma-Aldrich, ≥99%), $(NH_4)_6H_2W_{12}O_{40}{\cdot}xH_2O$ (Sigma-Aldrich, ≥99.0%), $(NH_4)_6Mo_7O_{24}{\cdot}4H_2O$ (Sigma-Aldrich, ≥99.0%), NH_4VO_3 (Sigma-Aldrich, ≥99.0%), $Cu(NO_3)_2{\cdot}3H_2O$ (Sigma-Aldrich, ≥99.0%), $Fe(NO_3)_3{\cdot}9H_2O$ (Sigma-Aldrich, ≥98.0%), $Fe(NO_3)_2{\cdot}6H_2O$ (Sigma-Aldrich, ≥98.0%), $Ni(C_2H_3O)_2{\cdot}4H_2O$ (Sigma-Aldrich, 98.0%), and $Ni(NO_3)_2{\cdot}6H_2O$ (Sigma-Aldrich, ≥97.0%).

The active carbon was Daihope 009. The silica was supplied by Saint-Gobain NorPro (type SS6*138 with a purity of ≥99.5%). Also, the ZrO_2 was supplied by Saint-Gobain NorPro (type SZ6*152 with an impurity of 3.3% SiO_2). The alumina was supplied by Sasol (type Puralox TH 100/150). The spinel was produced from the Al_2O_3 by mixing stoichiometric amounts of Al_2O_3 and MgO and calcination of the mixture at 900 °C; the product was confirmed to be a mixed oxide ($MgAl_2O_4$) by X-ray diffraction (XRD). CeO_2 and CeO_2-ZrO_2 were supplied by AMR Ltd. CeO_2-ZrO_2 was confirmed by XRD to be a mixed oxide. Before impregnation, all supports were crushed and sieved.

Incipient wetness impregnation was made by initially dissolving the corresponding amount of precursors in deionized water equivalent to the pore volume of the support and then mixing with the support. All precursors described above were sufficiently water-soluble. After impregnation, the samples were dried at 110 °C for at least 12 h and then calcined at 400 °C with a heating rate of 10 °C/min and a holding time of 4 h. The catalysts with carbon supports were calcined in nitrogen, while other catalysts were calcined in air.

For example, NiCu/SiO_2 was prepared by dissolving 3.80 g of $Cu(NO_3)_2{\cdot}3H_2O$ and 4.95 g of $Ni(NO_3)_2{\cdot}6H_2O$ in 8 mL of deionized water and impregnation of this solution on 8 g of dried SiO_2.

The Ni-V_2O_5 catalysts were made by initially impregnating the support with vanadium, drying the catalyst, and then impregnating it with nickel nitrate. NH_4VO_3 was dissolved by using additionally oxalic acid (Sigma-Aldrich, ≥99.0%) in a molar ratio of 1:2 (V:oxalic acid).

Cu/ZnO/Al_2O_3 was prepared according to the method of Baltes et al.[19] An aqueous solution of $Cu(NO_3)_2{\cdot}3H_2O$ (0.6 mol/L, Sigma-Aldrich, ≥99%), $Zn(NO_3)_2{\cdot}6H_2O$ (0.3 mol/L, Sigma-Aldrich, ≥99%), and $Al(NO_3)_3{\cdot}9H_2O$ (0.1 mol/L, Sigma-Aldrich, ≥98%) was coprecipitated with a solution of Na_2CO_3 (1 mol/L, Sigma-Aldrich, ≥99%) for 1 h. During the precipitation process, the pH was maintained at 7 ± 0.1 and the temperature was kept at 60 °C. Afterward, the precipitate was filtered and washed with demineralized water followed by drying overnight at 80 °C and calcining at 300 °C under air for 3 h.

NiO-MoO_3/Al_2O_3 and CoO-MoO_3/Al_2O_3 catalysts were obtained from Haldor Topsøe A/S. Ru/C, Pd/C, and Pt/C were obtained from Sigma-Aldrich.

Table 1 also summarizes the theoretical loadings, particle sizes, specific surface areas, and pretreatment conditions of the different catalysts.

2.2. Catalyst Testing. The screening experiments were performed in a 300 mL batch reactor (Parr, type 4566) made from Hastelloy C steel. One gram of catalyst was loaded in the reactor, and then 50 g of phenol (Sigma-Aldrich, ≥99%) was added. The mixture was stirred with a propeller at 380−390 rpm throughout the experiment and heated to 275 °C in a hydrogen atmosphere, giving a final pressure of 100 bar. The heating rate was ∼12.5 °C/min. During the experiments, hydrogen was added continuously to maintain the pressure. To stop the experiment, the reactor was placed in an ice bath (cooling rate of ∼25−50 °C/min). The start of the experiment was taken as the time when the heater was turned on and the end of the experiment when the reactor was lowered into the ice bath. The resultant product was filtered by suction filtration to separate the product liquid and catalyst.

Catalytic activity measurements over oxide and methanol synthesis catalysts were performed with a mixture of 10 g of phenol in 40 mL of deionized water as feedstock, because low levels of conversion were observed in this series of experiments. Addition of water was required as a solvent for phenol, as the reactant is solid at room temperature and therefore difficult with which to work in the product separation and gas chromatography (GC) analysis.

In a blank experiment without catalyst, 10 g of phenol and 40 mL of H_2O were allowed to react for 4 h at 275 °C and 100 bar. Almost no catalytic activity was seen in this case as a conversion of 0.3% was observed. Thus, the reactor was hardly catalytically active and did not influence the experiments. The blank experiment was repeated occasionally to ensure that the reactor was not contaminated over time.

By 3-fold repetition of a hydrodeoxygenation experiment with Ni/SiO_2, it was found that this procedure typically had an uncertainty in the measured yields of ±2 mol %, corresponding to <5% as the relative standard deviation. Overall, the repeatability of the experiments was good.

In some cases, shorter experiments had to be performed not to reach 100% conversion. Here the batch reactor was initially heated without its contents being stirred. It was assumed that the extent of the reaction was low in the heating phase because of the mass transfer restriction of hydrogen in such systems.[20] This was supported by the observation that no hydrogen was consumed in the heating phase. When the desired temperature was reached, the stirring was started at 380−390 rpm and the experiment could be performed at close to isothermal conditions. This made it possible to measure the activity in short-term (5−30 min) experiments.

As specified in Table 1, some of the catalysts were pretreated in hydrogen to reduce the active metals. This was done in a continuous flow setup, where the sample was treated at the specified temperature in a 50:50 mixture of hydrogen and nitrogen at a total flow of 500 NmL/min. Temperature-programmed reduction by hydrogen (H_2-TPR) was used to

dx.doi.org/10.1021/cs400266e | ACS Catal. 2013, 3, 1774−1785

evaluate the required reduction temperature, and XRD confirmed that the catalysts were reduced under the specified conditions.

2.3. Product Analysis. Analysis of the liquid product was performed with a Shimadzu GCMS/FID-QP2010UltraEi instrument fitted with a Supelco Equity-5 column and equipped with a mass spectrometer (MS) for product identification and a flame ionization detector (FID) for quantification. External standards were prepared for phenol, cyclohexanol, cyclohexanone, and cyclohexane using ethanol as a solvent. The concentrations of the remaining peaks were calculated from the FID on the basis of the effective carbon number method,[21] where the concentration of a compound is found to be

$$C_i = C_{\text{ref}} \frac{A_i}{A_{\text{ref}}} \frac{\nu_{\text{eff,ref}}}{\nu_{\text{eff},i}} \tag{2}$$

where C is the concentration, A the area of the peak in the FID spectrum, and ν_{eff} the effective carbon number. Index i refers to the compound with the unknown concentration, and index ref refers to a reference compound where the concentration is known. In all calculations with this formula, cyclohexanol was used as a reference. The effective carbon number was obtained from the review of Schofield.[21]

The conversion, X, was calculated as

$$X = \left(1 - \frac{n_{\text{phenol}}}{n_{0,\text{phenol}}}\right) \times 100\% \tag{3}$$

where n_{phenol} is the moles of phenol after reaction and $n_{0,\text{phenol}}$ the moles of phenol prior to reaction.

The yields (Y_i) of relevant products were calculated as

$$Y_i = \frac{\nu_i n_i}{6 n_{0,\text{phenol}}} \times 100\% \tag{4}$$

where n_i is the moles of product i after reaction and ν_i the number of carbon atoms in compound i.

The carbon balance was evaluated in all experiments by comparing the carbon initially in the reactor to the carbon measured in the product and on the catalyst:

$$\Delta C = \left(\frac{\sum_i \nu_i n_i - 6 n_{0,\text{phenol}}}{6 n_{0,\text{phenol}}}\right) \times 100\% \tag{5}$$

where ΔC is the carbon deviation in percent and n_i the moles of compound i. All compounds identified in the GC analysis were included in the carbon balance. Generally, the carbon balance was closed within 10%, but in many experiments, almost complete closure was achieved; this will be discussed later.

All calculations of X, Y_i, and ΔC were corrected for loss of mass from transferring and filtration processes, which was quantified as the average of a number of blank tests.

2.4. Catalyst Characterization. A Quantachrome iQ2 instrument was used for measurement of the specific surface area on the basis of BET theory.[22] Nitrogen at its boiling point was used in the p/p_0 range from 0.05 to 0.3 to construct a seven-point BET plot. Generally, all the tested supports had surface areas on the same order of magnitude; only the carbon support had a significantly larger surface area (see Table 1).

Temperature-programmed reduction by hydrogen was performed for selected catalysts on a Netzsch STA 449 F1 Jupiter ASC thermogravimetric analyzer to identify the required temperature for complete reduction of the supported metal. The analysis was performed on the basis of changes in mass, and the total mass applied was on the order of 20−40 mg. Five volume percent hydrogen in nitrogen was added at a flow of 100 NmL/min, and the samples were heated at a rate of 5 °C/min to 300 °C, at a rate of 1 °C/min from 300 to 500 °C, and at a rate of 5 °C/min from 500 to 700 °C.

NH_3-TPD was performed with an Autochem II 2920 apparatus. Here ∼0.1 g portions of the samples were initially heated to 500 °C in a 50 mL/min He flow and then cooled to 100 °C. At this point, the samples were saturated with a 50 mL/min NH_3 flow for 120 min. Desorption of NH_3 was hereafter measured by flushing with a 50 mL/min He flow while heating the sample at a rate of 5 °C/min to 500 °C.

X-ray diffraction (XRD) was measured with a PANalytical X'Pert PRO instrument using a rotating copper anode X-ray source at 40 kV and 30 mA, a nickel filter, and automatic antiscatter and divergence slits. The 2Θ angle was scanned from 12° to 120° in increments of 0.00656° with 45.9 s per step. The mean coherent-scattering domain (CSD) size was derived from reflection half-widths using the Selyakov−Scherrer formula.[23] All samples were analyzed as prepared powders.

3. KINETICS OF PHENOL HDO

To determine the activity of the catalysts on a quantitative basis, a kinetic model was developed. In the following, this model is presented as a basis for the later discussion.

The time-dependent development of the conversion of phenol and the yields of cyclohexanone, cyclohexanol, and cyclohexane in an experiment with a Ni-V_2O_5/SiO_2 catalyst at 250 °C and 100 bar is shown in Figure 2. At first, phenol was converted to primarily cyclohexanol. This yield was maximal after reaction for approximately 3.5 h. The cyclohexane yield, on the other hand, increased continuously throughout the experiment, with an increasing rate toward the end.

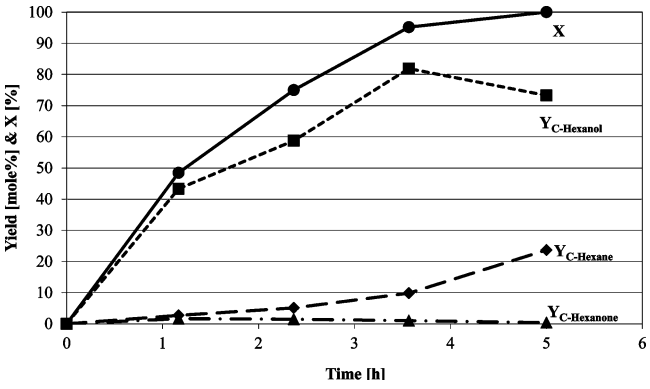

Figure 2. Conversion of phenol (X) and yields of cyclohexanone, cyclohexanol, and cyclohexane as a function of time over a Ni-V_2O_5/SiO_2 catalyst. The experiments were conducted with 1 g of catalyst in 50 g of phenol. T = 250 °C, and P = 100 bar.

The data in Figure 1 indicate a reaction mechanism at 250 °C in which hydrogenation of the aromatic ring occurs as a first step followed by deoxygenation, with cyclohexanol as the intermediate product and cyclohexane as the final product. Also, cyclohexanone and cyclohexene were observed in small amounts. The cyclohexanone yield reached a maximum of 1.7% after 1 h and then steadily decreased (cf. Figure 2). The cyclohexene yield was even less and on the order of 0.01%.

dx.doi.org/10.1021/cs400266e | ACS Catal. 2013, 3, 1774−1785

Shuikin and Erivanskaya[24] suggested that hydrogenation of phenol over Ni catalysts produces cyclohexanone as the primary product; however, the subsequent hydrogenation of cyclohexanone to cyclohexanol proceeds at a much higher rate, and therefore, cyclohexanone is seen in only low yields. Similarly, cyclohexene is formed through dehydration of cyclohexanol followed by quick hydrogenation to cyclohexane. Overall, the observations from Figure 2 and previous literature for nickel catalysts,[24] Pd/C,[25,26] Pt/C,[27] Ni/HZSM-5,[28] and Ni-MoS_2/Al_2O_3[29] suggest the reaction scheme depicted in Figure 3 with solid arrows. To verify this, measurements were

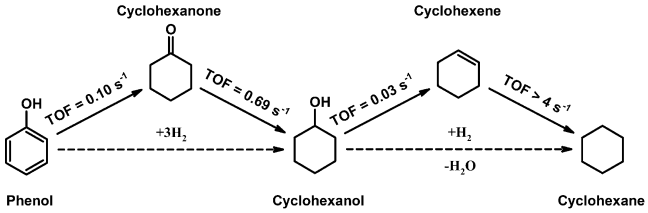

Figure 3. Observed reaction path for HDO of phenol. Solid arrows indicate main pathways, while dashed arrows show the effective conversion steps in the kinetic model. Indicated rates are from measurements with a 5 wt % Ni/ZrO_2 catalyst at 275 °C and 100 bar in the batch reactor setup. The estimations of the individual turnover frequencies (TOF) are supplied in the Supporting Information.

performed over a Ni/ZrO_2 catalyst to quantify the rate of the four steps (see the Supporting Information). This is shown in Figure 3 as the turnover frequency (TOF) in each step. Hydrogenation of cyclohexanone and hydrogenation of cyclohexene were significantly faster reactions than hydrogenation of phenol and dehydration of cyclohexanol. Hence, only low yields of cyclohexanone and cyclohexene should be expected.

From the data in Figures 2 and 3, deoxygenation appears to take place more readily from a saturated ring than from an unsaturated ring, which has also been shown elsewhere.[1,8,30] This is related to the dissociation energy of the C−O bond in alcohols,[31] which decreases in the following order:

$$\begin{aligned} &\text{aomatic alcohol (469 kJ/mol)} \\ &\gg \text{secondary alcohol (385 kJ/mol)} \\ &\approx \text{primary alcohol (383 kJ/mol)} \\ &\approx \text{tertiary alcohol (379 kJ/mol)} \end{aligned} \quad (6)$$

The data clearly show that the aromatic alcohol (i.e., phenol) has an ∼100 kJ/mol higher bond dissociation energy than the secondary alcohol (as cyclohexane), and the deoxygenation can therefore more readily take place from the cyclohexanol compared to the phenol as the C−O bond is markedly weakened.

Because the rates of hydrogenation of both cyclohexanone and cyclohexene are relatively fast and the yields of these compounds are low, the effective reaction scheme can be described by the dotted arrows in Figure 3, which results in the following two overall main reactions:

$$\text{phenol} + 3H_2 \rightarrow \text{cyclohexanol} \quad (I)$$

$$\text{cyclohexanol} + H_2 \rightarrow \text{cyclohexane} + H_2O \quad (II)$$

Assuming first-order dependency of the hydrocarbon compounds leads to the following rate expressions:

$$r_1 = k_1 C_{\text{phenol}} P_{H_2}^n \quad (7)$$

$$r_2 = k_2 C_{\text{C-hexanol}} P_{H_2}^m \quad (8)$$

where r_i is the rate of reaction i, k_i is the rate constant of reaction i, C_i is the concentration of either phenol or cyclohexanol, and n and m are the reaction orders of hydrogen in reactions I and II, respectively. The assumption of first-order kinetics with respect to the hydrocarbons is made in the absence of a better estimate. As all the experiments were performed with the same and constant pressure of hydrogen, the hydrogen pressure can be included in the rate constant and thereby give the following lumped rate expressions:

$$r_1 = k_1' C_{\text{phenol}} \quad (9)$$

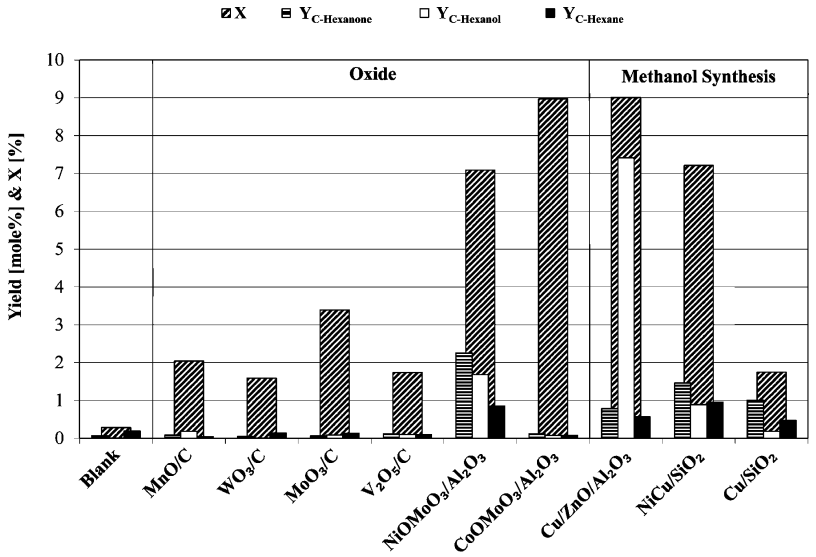

Figure 4. Conversion of phenol (X) and yields of cyclohexanone, cyclohexanol, and cyclohexane from experiments with different types of oxide catalysts ("Oxide") and methanol synthesis catalysts ("Methanol Synthesis") and for the blank experiment. The experiments were conducted with 0.5 g of catalyst in 10 g of phenol and 40 mL of water. T = 275 °C, and P = 100 bar. The reaction time was 4 h.

dx.doi.org/10.1021/cs400266e | ACS Catal. 2013, 3, 1774−1785

$$r_2 = k_2' C_{\text{C-hexanol}} \quad (10)$$

where k_1' is the rate constant for the hydrogenation reaction and k_2' the rate constant for the deoxygenation reaction. The rate expressions in eqs 9 and 10 were combined with the batch reactor design equation[32] to allow determination of k_1' and k_2' from the experimental data and a quantitative comparison of the different catalysts.

A thorough description of the derivation of the model, the assumptions made, and the validation of the model can be found in the Supporting Information.

4. RESULTS AND DISCUSSION

4.1. Oxide and Methanol Synthesis Catalysts. The results from testing the oxide catalysts at 275 °C and 100 bar are shown in Figure 4 in terms of the yields of cyclohexanone, cyclohexanol, and cyclohexane, and the conversion of phenol. None of the catalysts achieved a conversion of >10%. The NiO-MoO_3/Al_2O_3 catalyst showed some hydrogenation activity with a yield of 4% oxygenated cyclohexanes. However, the activity for HDO over this catalyst was low, with a yield of cyclohexane of only 0.9%.

Table 2 gives a summary of the performance of the catalysts. The carbon balances of the experiments were reasonably well closed and in most cases were on the order of −2%. Only the CoO-MoO_3/Al_2O_3 catalyst had a larger carbon deviation of −8.5%. As the conversion of phenol was 9% on this catalyst, it could indicate that this catalyst mainly was active for cracking.

Table 2. Overview of the Results from Different Oxide Catalysts and Methanol Synthesis Catalysts[a]

catalyst	k_1' (mL kg_{cat}^{-1} min^{-1})	k_2' (mL kg_{cat}^{-1} min^{-1})	ΔC (%)
blank	–	–	0.0
MnO/C	1	7	−1.1
WO_3/C	1	10	−1.4
MoO_3/C	2	4	−3.1
V_2O_5/C	1	3	−1.4
NiO-MoO_3/Al_2O_3	5	20	−2.2
CoO-MoO_3/Al_2O_3	6	0	−8.5
Cu/ZnO/Al_2O_3	8	10	−0.2
NiCu/SiO_2	7	28	−3.9
Cu/SiO_2	1	50	−0.1

[a] k_1' is the rate constant for hydrogenation. k_2' is the rate constant for deoxygenation. ΔC is the deviation in the carbon balance. The experiments were conducted with 0.5 g of catalyst in 10 g of phenol and 40 mL of water. T = 275 °C, and P = 100 bar. The reaction time was 4 h.

Prasomsri et al.[33] did observe HDO activity of bulk V_2O_5, Fe_2O_3, CuO, WO_3, and MoO_3 catalysts in a continuous flow reactor for acetone deoxygenation in the gas phase at atmospheric pressure and 400 °C, with MoO_3 performing the best. In contrast to their study for which temperatures of 400 °C were required to deoxygenate anisole, much lower temperatures were used in the current screening. The higher temperature requirement is probably linked to the inability of the catalyst to hydrogenate the anisole and instead being forced to break the stronger C−O bond of the aromatic alcohol compared to the saturated form, as discussed in section 3 (see eq 6).

Figure 4 also shows the results of the screening of the methanol synthesis catalysts (Cu/SiO_2, NiCu/SiO_2, and Cu/ZnO/Al_2O_3). This group of catalysts also had a low activity. Cu/ZnO/Al_2O_3 had a conversion of ∼9% but primarily was selective toward hydrogenation, with cyclohexanol and cyclohexanone constituting 91% of the product. NiCu/SiO_2 had a conversion of 7%, but according to the carbon balance (cf. Table 2), half of the measured conversion was not accounted for.

Among these catalysts, Cu/ZnO/Al_2O_3 was the best performing, with the highest conversion and a good closure of the carbon balance (ΔC = −0.2%). However, as the product primarily was cyclohexanol, the potential of this catalyst seems limited in the context of HDO.

Ardiyanti et al.[34] previously investigated Cu/Al_2O_3 and NiCu/Al_2O_3 catalysts at varying Ni/Cu ratios for HDO of anisole at 300 °C and 10 bar in a continuous flow reactor. In these studies, it was observed that the pure Cu catalyst was unable to perform HDO of the anisole, as the only product was phenol. For NiCu/Al_2O_3, the best catalyst was obtained with a 8:1 Ni:Cu weight ratio. In agreement with this, we also observed the improved activity of the NiCu/SiO_2 (with a Ni:Cu ratio of 1) catalyst relative to that of Cu/SiO_2, but the activity of NiCu/SiO_2 was not optimized as in the work of Ardiyanti et al.[34] The results indicate that the Ni loading has to be markedly higher than the Cu loading to achieve good HDO activity.

In summary, the apparent order of activity for the tested oxide and methanol catalysts was as follows:

$$\text{Cu/ZnO/Al}_2\text{O}_3 \approx \text{NiO-MoO}_3\text{/Al}_2\text{O}_3 \approx \text{NiCu/SiO}_2 > \text{Cu/SiO}_2 > \text{MnO/C, WO}_3\text{/C, V}_2\text{O}_5\text{/C, CoO-MoO}_3\text{/Al}_2\text{O}_3$$

Commonly, none of the catalysts achieved high conversion under these conditions because of their inability to hydrogenate the aromatic ring of phenol (cf. Table 2).

4.2. Reduced Noble Metal Catalysts. In the experiments with reduced noble metal catalysts, higher conversions were observed compared to the oxide and methanol synthesis catalysts. Thus, pure phenol was used for these experiments, as this gave consistency. The reaction temperature and pressure were kept the same.

Figure 5 summarizes the conversion of phenol and the yields of cyclohexanol, cyclohexane, and dicyclohexyl ether from the experiments with noble metal catalysts. All the catalysts gave complete conversion of the phenol through a relatively fast hydrogenation reaction to cyclohexanol. The subsequent HDO more favorably took place on the ruthenium catalyst than on the platinum and palladium catalysts. The ruthenium catalyst provided a yield of 52% cyclohexane relative to 1 and 11% on the platinum and palladium catalysts, respectively. The palladium catalyst furthermore had a high yield of dicyclohexyl ether of 21%, i.e., higher than the cyclohexane yield.

Table 3 summarizes the kinetic parameters of the reactions. The hydrogenation rate constants (k_1') were on the same order of magnitude for Ru/C and Pd/C, but Pt/C had a rate of hydrogenation ∼1 order of magnitude higher. In general, all three catalysts, however, were good hydrogenation catalysts, achieving 100% conversion of the phenol in the 5 h experiments.

With regard to the hydrodeoxygenation step (k_2'), the catalytic activity of Ru/C was 1 order of magnitude higher than that of Pd/C and 2 orders of magnitude higher than that

dx.doi.org/10.1021/cs400266e | ACS Catal. 2013, 3, 1774−1785

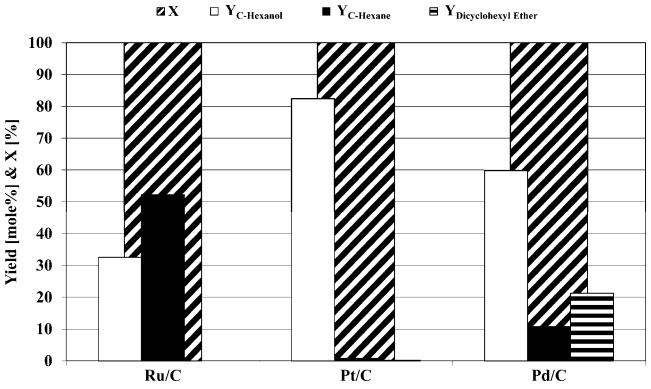

Figure 5. Conversion of phenol (X) and yields of cyclohexanol, cyclohexane, and dicyclohexyl ether from experiments with different types of reduced noble metal catalysts. The experiments were conducted with 1 g of catalyst in 50 g of phenol. T = 275 °C, and P = 100 bar. The reaction time was 5 h.

Table 3. Overview of the Results from the Reduced Noble Metal Catalysts[a]

catalyst	d_M (nm)	k_1' (mL kg_{cat}^{-1} min^{-1})	k_2' (mL kg_{cat}^{-1} min^{-1})	ΔC (%)
Ru/C	7	1950[b]	115	−10.8
Pt/C	4	31200[c]	1	−11.8
Pd/C	6	1840[d]	19	−6.1

[a] d_M is the metal crystallite size measured by XRD. k_1' is the rate constant for hydrogenation. k_2' is the rate constant for deoxygenation. ΔC is the deviation in the carbon balance. The experiments were conducted with 1 g of catalyst in 50 g of phenol. T = 275 °C, and P = 100 bar. The reaction time was 5 h. [b]Determined from an 18 min isothermal experiment at 275 °C with 50% phenol conversion. [c]Determined from a 10 min isothermal experiment at 275 °C with 99.8% phenol conversion. [d]Determined from a 16 min isothermal experiment at 275 °C with 44% phenol conversion.

of Pt/C. This analysis does not take into account the fact that the primary part of the deoxygenation for the Pd/C catalyst was taking place through the ether-forming reaction, and k_2' is therefore not completely descriptive of the affinity for deoxygenation on Pd/C. Nevertheless, the trend is clear.

The carbon balance in Table 3 shows that all the tested catalysts lacked on the order of 5−10% carbon. Analysis of the gas phase from the Ru/C experiment by sampling in a gas bag and then analyzing on a GC-TCD instrument showed the presence of CO_2, CH_4, and CO. Furthermore, traces of pentane, hexane, ethanol, methanol, and acetone could be identified in the oil phase. This shows that cracking reactions take place on the Ru/C catalyst. It has previously been shown that Ru/C can produce CH_4 and CO_2 from guaiacol at temperatures above 250 °C.[35] Elliott and Hart[35] linked the production of these gases to aqueous phase re-forming, which for Ru/C has been shown to occur under similar conditions.[36]

Overall, the apparent order of activity for deoxygenation for the tested noble metal catalysts for HDO of phenol was found to be

$$\text{Ru/C} > \text{Pd/C} > \text{Pt/C}$$

In agreement with this, Elliott and Hart[35] found Ru/C to be a better catalyst than Pd/C for the conversion of guaiacol in a batch reactor. Wildschut et al.[37] identified Ru/C and Pd/C as better performing catalysts compared to Pt/C for bio-oil HDO in a batch reactor. Lee et al.[38] identified Ru/SiO_2-Al_2O_3 as the best performing catalyst for guaiacol HDO in comparison to platinum and palladium. Adriyanti et al.[39] found Pd/ZrO_2 to be a better catalyst for bio-oil HDO in a batch reactor compared to Pt/ZrO_2. Thus, these results for HDO over noble metal catalysts are in good agreement with the literature, which all point toward ruthenium being one of the best performing noble metals for HDO and with Pd being more efficient than Pt. The kinetic model revealed that the reason for this is that Pt is a relatively poor deoxygenation catalyst but a very good hydrogenation catalyst.

The reason for ruthenium being the best performing noble metal could be correlated to the affinity of the metals to bind oxygen. Nørskov et al.[40] showed through density functional theory (DFT) calculations that the binding energies of oxygen relative to water (ΔE_O) were −0.01, 1.53, and 1.57 eV on Ru, Pd, and Pt, respectively. Thus, ruthenium has the strongest binding energy with respect to oxygen, and platinum the weakest, which correlates with the affinity for performing deoxygenation.

In this work, the effect of support was not investigated, but previous work has shown that the type of support can significantly increase the activity of noble metal catalysts. Lee et al.[38] tested noble metal catalysts on C, Al_2O_3, and SiO_2-Al_2O_3 for guaiacol HDO at 250 °C and 40−70 bar in a batch reactor. Their work showed that the activity of all the supported noble metal catalysts was improved in the order of increasing support acidity, i.e., an apparent order of activity of NM/SiO_2-Al_2O_3 > NM/Al_2O_3 > NM/C, where NM is a noble metal. Similar, Foster et al.[41] also observed increasing catalytic activity for HDO of *m*-cresol over platinum catalysts with increasing acidity of the support at 260 °C and 1 atm in a packed bed reactor setup. Both studies point toward the possibility that the use of an acidic support can increase the activity of the noble metal catalysts. The role of support is discussed further in section 4.3.3.

4.3. Reduced Non-Noble Metal Catalysts. *4.3.1. Reduction Temperature.* Prior to the activity tests of the non-noble metal catalysts, the required reduction temperatures were determined by H_2-TPR. Table 4 summarizes the results of these measurements, showing the temperature intervals where the reduction took place.

For the nickel-based catalysts, the theoretical mass loss is 1.4 wt % for a nickel loading of 5 wt %, assuming that all nickel is reduced from NiO to Ni. Generally, the measured mass loss

Table 4. Results from H_2-TPR of the Reduced Non-Noble Metal Catalysts[a]

catalyst	start (°C)	end (°C)	mass loss (wt %)	theoretical mass loss
Co/SiO_2	260	520	1.0	1.4
Ni/SiO_2	305	365	1.4	1.4
Ni/Al_2O_3	310	505	0.9	1.4
Ni/CeO_2	280	335	1.3	1.4
Ni/CeO_2-ZrO_2	295	500	1.2	1.4
Ni/ZrO_2	310	485	1.4	1.4
Ni/$MgAl_2O_4$	305	500	0.6	1.4
Ni/C	360	505	1.1	1.4
Ni-V_2O_5/SiO_2	300	390	3.1	5

[a]Start and end indicate the temperature interval over which reduction was observed. Conditions: gas, 5% H_2 in N_2; flow rate of , 100 NmL/min; heating ramp, 5 °C/min to 300 °C, 1 °C/min from 300 to 500 °C, and 5 °C/min from 500 to 700 °C; sample amount, 20−40 mg.

dx.doi.org/10.1021/cs400266e | ACS Catal. 2013, 3, 1774−1785

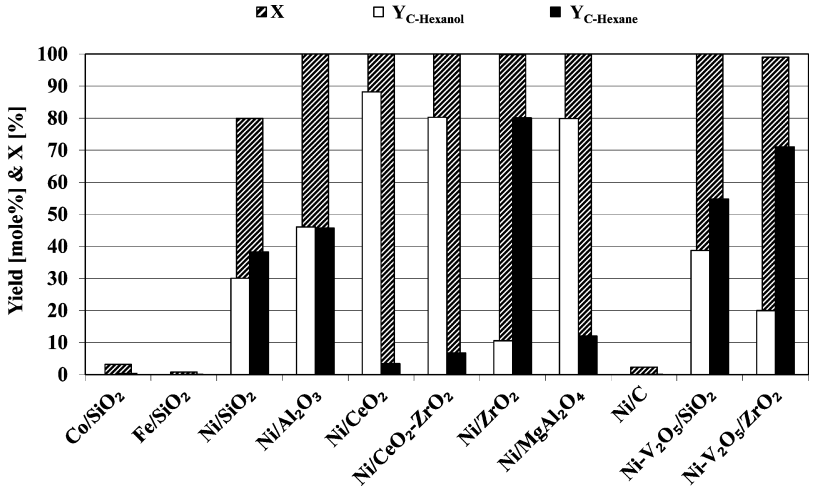

Figure 6. Conversion of phenol (X) and yields of cyclohexanol and cyclohexane from experiments with different types of reduced non-noble metal catalysts. The experiments were conducted with 1 g of catalyst in 50 g of phenol. T = 275 °C, and P = 100 bar. The reaction time was 5 h.

was close to the theoretical mass loss. The largest deviation was seen in the case of Ni/Al_2O_3 and $Ni/MgAl_2O_4$, with measured mass losses of 0.9 and 0.6 wt %, respectively. For these catalysts, the XRD analyses of the used catalysts revealed that the nickel to some extent was interacting with the supports, forming a mixed oxide with the alumina or spinel. These oxides have been shown to retard reduction, resulting in the observed lower degree of reduction.[42]

For $Ni\text{-}V_2O_5/SiO_2$, complete reduction of the nickel and vanadium into NiV/SiO_2 would result in a theoretical mass loss of 5 wt %. However, only a 3.1 wt % weight loss was observed, showing that the catalyst was not completely reduced and probably still contained vanadium in the form of oxides even at 700 °C.

Overall, the identified end temperatures from the TPR analyses are judged to be sufficient for complete reduction. The actual reduction temperature, which is given in Table 1, was set higher for the individual samples to ensure complete reduction.

4.3.2. Reduced Non-Noble Metals. Three reduced non-noble metals were tested: Ni/SiO_2, Co/SiO_2, and Fe/SiO_2. These were chosen on the basis of their known hydrogenation activity in other processes.[43−46] Figure 6 shows the comparison between the activities of these three catalysts. Ni/SiO_2 was the most active catalyst with a conversion of 80%, compared to 3.2 and 0.8% for Co/SiO_2 and Fe/SiO_2, respectively.

The kinetic data for the three catalysts are listed in Table 5. The k_1' rate constants of Co/SiO_2 and Fe/SiO_2 were 5 and 1 mL kg_{cat}^{-1} min^{-1}, respectively, showing that Co/SiO_2 was the better hydrogenation catalyst of the two. However, k_1' was 2 orders of magnitude larger for Ni/SiO_2 in comparison. k_2' was on the same order of magnitude for Co/SiO_2 and Fe/SiO_2, but significantly larger for Ni/SiO_2, as seen from Table 5.

XRD of the spent Ni/SiO_2, Co/SiO_2, and Fe/SiO_2 showed the active metals to be reduced and to have similar metal crystallite sizes.

In summary, the apparent order of activity for the three non-noble metal catalysts is

$$Ni/SiO_2 \gg Co/SiO_2 > Fe/SiO_2 \quad (11)$$

The better performance of Co/SiO_2 compared to that of Fe/SiO_2 is due to a better activity for hydrogenation on this catalyst. Finding similar results, Filley and Roth[47] investigated cobalt and iron supported on alumina for HDO of guaiacol at atmospheric pressure and 350 °C and did not find any notable activity. Yakovlev et al.[11] investigated both cobalt and nickel catalysts for HDO of anisole at 300 °C and 10 bar of hydrogen and found that Co/SiO_2 was practically inactive compared to Ni/SiO_2, which is similar to the results of this work.

Table 5. Overview of the Results from Reduced Non-Noble Metal Catalysts[a]

catalyst	d_M (nm)	k_1' (mL kg_{cat}^{-1} min^{-1})	k_2' (mL kg_{cat}^{-1} min^{-1})	ΔC (%)	NH_3 adsorption (μmol/g_{cat}) weak	strong
Co/SiO_2	12	5	52	−2.6	–	–
Fe/SiO_2	12	1	64	−0.3	–	–
Ni/SiO_2	9	230	159	−4.2	40	–
Ni/Al_2O_3	7	3200[b]	100	−0.5	210	220
Ni/CeO_2	8	21800[c]	6	−8.0	–	400
$Ni/CeO_2\text{-}ZrO_2$	6	10500[d]	13	−6.3	–	250
Ni/ZrO_2	7	1010[e]	361	−1.1	210	210
$Ni/MgAl_2O_4$	10	6580[f]	25	−4.4	140	150
Ni/C	14	3	121[g]	−2.0	30	–
$Ni\text{-}V_2O_5/SiO_2$	–	1160	136	−0.8	60	–
$Ni\text{-}V_2O_5/ZrO_2$	–	701	256	−1.5	130	230

[a] d_M is the metal crystallite size measured by XRD. k_1' is the rate constant for hydrogenation. k_2' is the rate constant for deoxygenation. ΔC is the deviation in the carbon balance. NH_3 adsorption is the ammonia saturation measured by NH_3-TPD. The data are distinguished as weak and strong adsorption, with weak being the signal recorded for desorption peaks below 200 °C and strong being above. The experiments were conducted with 1 g of catalyst in 50 g of phenol. T = 275 °C, and P = 100 bar. The reaction time was 5 h. [b]Determined from a 13 min isothermal experiment at 275 °C with 54% phenol conversion. [c]Determined from a 10 min isothermal experiment at 275 °C with 98.7% phenol conversion. [d]Determined from a 15 min isothermal experiment at 275 °C with 95% phenol conversion. [e]Determined from a 15 min isothermal experiment at 275 °C with 26% phenol conversion. [f]Determined from a 10 min isothermal experiment at 275 °C with 74% phenol conversion. [g]Determined from a 4 h experiment at 275 °C with cyclohexanol as the feed instead of phenol.

4.3.3. Support Effect on Nickel Catalysts. With nickel having been identified as the best performing of the tested non-

dx.doi.org/10.1021/cs400266e | ACS Catal. 2013, 3, 1774−1785

noble metal catalysts, this was chosen for further investigation with respect to the influence of support.

Seven different types of supports of comparable specific surface areas (cf. Table 1), were tested and very different activities were observed, as summarized in Figure 6. Ni/C was the only catalyst with practically no activity and a conversion of only 2%. On the other hand, Ni/CeO_2, Ni/CeO_2-ZrO_2, and $Ni/MgAl_2O_4$ were very active for hydrogenation with conversions of 100%, but less active for deoxygenation with yields of cyclohexane of 4, 8, and 12%, respectively. Ni/Al_2O_3 had a high activity for both hydrogenation and deoxygenation with a conversion of 100% and a yield of 46% cyclohexane. Ni/SiO_2 gave a yield of cyclohexane on the same order of magnitude (38%) but was significantly less active for hydrogenation with a conversion of 80%. Ni/ZrO_2 was the overall best performing catalyst under these conditions with almost complete conversion of phenol (X = 99.8%) and a high selectivity toward cyclohexane ($Y_{C\text{-}hexane}$ = 83%).

The kinetic data in Table 5 show that Ni/CeO_2 had the highest hydrogenation rate constant (k_1') followed by Ni/CeO_2-ZrO_2. Both catalysts showed hydrogenation rate constants 1 order of magnitude higher than those of $Ni/MgAl_2O_4$, Ni/Al_2O_3, and Ni/ZrO_2, decreasing in that order. Ni/SiO_2 had a hydrogenation rate constant 2 orders of magnitude lower than that of Ni/CeO_2.

In contrast, the Ni/CeO_2 catalyst had practically no activity for deoxygenation. The deoxygenation activity of Ni/CeO_2-ZrO_2 and $Ni/MgAl_2O_4$ was 2−5 times larger than for Ni/CeO_2, but still low yields of cyclohexane were produced. Only Ni/ZrO_2, Ni/SiO_2, and Ni/Al_2O_3 had relatively high rates of deoxygenation, decreasing in that order. An interesting aspect of this is that Ni/SiO_2 had a higher rate constant for deoxygenation than Ni/Al_2O_3, but because Ni/Al_2O_3 had a higher rate of hydrogenation, the cyclohexane yield with the Ni/Al_2O_3 catalyst was higher than that with the Ni/SiO_2 catalyst.

Ni/SiO_2 and Ni/ZrO_2 were additionally tested as catalysts where the support had initially been promoted by vanadium before impregnation with nickel. The results of these experiments are also shown in Figure 6, while kinetic data are listed in Table 5. For $Ni\text{-}V_2O_5/SiO_2$ the rate of hydrogenation was significantly increased compared to that of the pure Ni/SiO_2 catalyst. The cyclohexane yield also increased, which was primarily caused by the increased rate of hydrogenation, as the rate of deoxygenation did not change between the $Ni\text{-}V_2O_5/SiO_2$ and Ni/SiO_2 catalysts (cf. Table 5). The $Ni\text{-}V_2O_5/ZrO_2$ catalyst performed slightly worse than the non-vanadium-doped catalyst, as both the yield of cyclohexane and the rate constants were lower. Overall, it was observed that addition of vanadium primarily influenced the hydrogenation rate of the catalyst.

The carbon balances listed in Table 5 show an adequate closure in most cases. The largest deviation was found for the Ce-containing supports, where 6−8% of the carbon was unrecovered. This indicates that either cracking or coke deposition could take place on these catalysts. On the other hand, for the two best performing catalysts, Ni/ZrO_2 and Ni/Al_2O_3, the carbon balance deviation was on the order of 1%, indicating that these catalysts were less prone to coke deposition. In general, better closure of the carbon balance was found for the nickel-based catalysts than for the noble metal catalyst (cf. Tables 3 and 5), showing that these catalysts have a weaker tendency to cause cracking.

NH_3-TPD was performed, giving information about the total amount of available acid sites on the catalysts (see Table 5). The total acidity of the supports decreases in the following order:

$$Ni/Al_2O_3 \geq Ni/ZrO_2 \geq Ni/CeO_2 > Ni\text{-}V_2O_5/ZrO_2 > Ni/MgAl_2O_4 > Ni/CeO_2\text{-}ZrO_2 \gg Ni\text{-}V_2O_5/SiO_2 > Ni/SiO_2 > Ni/C$$

Via comparison of this to the apparent order of activity discussed above (or see Table 5), it follows that the amount of available acid sites (as measured by NH_3-TPD) and the HDO activity are not directly correlated. Most notable is Ni/SiO_2, which practically contains no acid sites but is found to be one of the three best HDO catalysts (of the investigated nickel catalysts). However, comparing only the rate constant for hydrogenation to the acidity gives some consistency as it is seen that the poor hydrogenation catalysts (Ni/SiO_2 and Ni/C) have very little acidity, while the catalysts with better hydrogenation affinity all have higher acidity. However, the acidity measurements do not reveal the true acidic nature of the catalyst under experimental conditions, as the reducing atmosphere in the experiments will result in an increased level of formation of oxygen vacancy sites and thereby acid sites.[48−51] A better understanding of this is gained by plotting the hydrogenation activity relative to the metal−oxygen bond strength [$E_{(M-O)}$] of the support, as shown in Figure 7. This

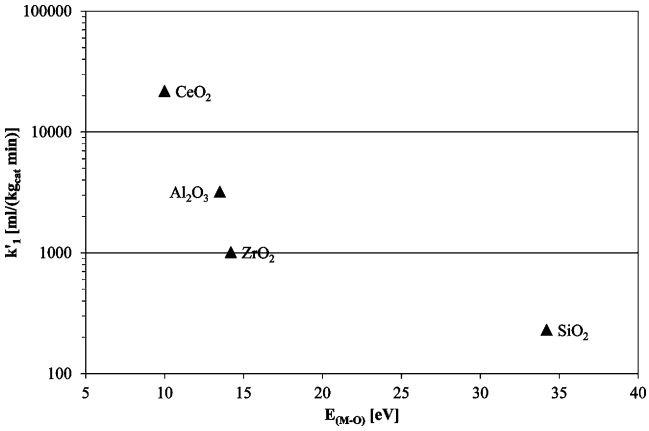

Figure 7. Hydrogenation activity as a function of the metal−oxygen bond strength [$E_{(M-O)}$] of the pure support. Only hydrogenation rate constants for nickel catalysts supported on pure oxides from Table 5 are plotted. $E_{(M-O)}$ data from ref 53.

reveals that oxide supports with low metal−oxygen bond energy had the highest activity for hydrogenation. Low M−O bond energies can be linked to the tendency for oxygen vacancy site generation in the oxide,[52,53] and these vacancy sites will function as Lewis acid sites.[51,53] Thus, the best performing hydrogenation catalyst is therefore the catalyst with the strongest tendency to form Lewis acid sites in the oxide structure that is most likely on the supports with the lowest metal−oxygen bond energy. Because of this effect, introducing V_2O_5 to a SiO_2 support causes formation of more vacancy sites because of the lower metal−oxygen bond energy of V_2O_5 (12.3 eV) compared to that of SiO_2 (34.2 eV) and thereby increases the hydrogenation activity (cf. Table 5). In contrast, doping ZrO_2 with V_2O_5 does not induce any large changes as the

dx.doi.org/10.1021/cs400266e | ACS Catal. 2013, 3, 1774−1785

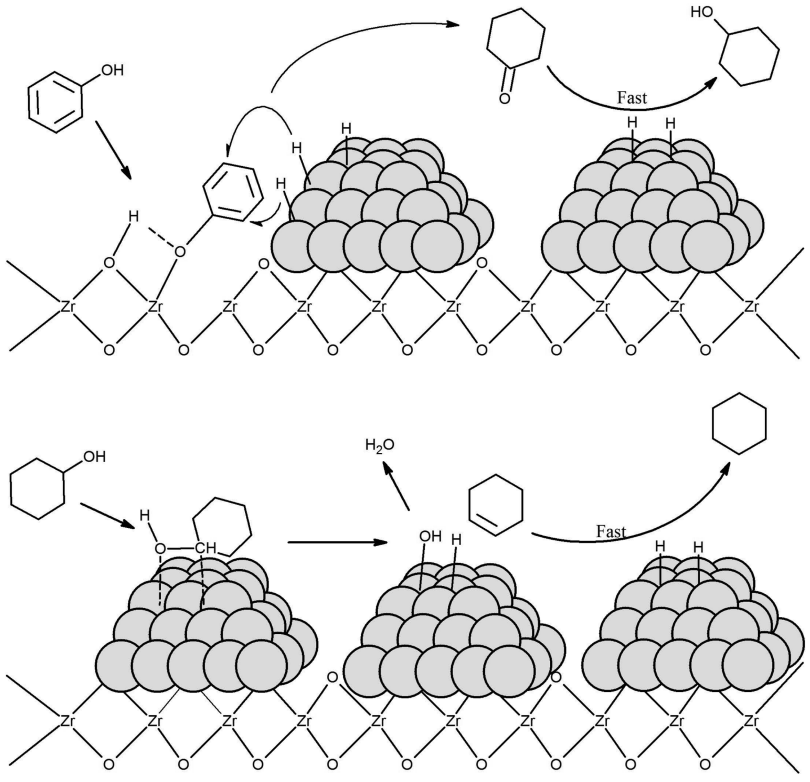

Figure 8. Proposed reaction mechanism for HDO of phenol over an oxide-supported nickel catalyst (here Ni/ZrO_2). Gray spheres represent nickel atoms.

metal−oxygen bond energies are relatively close (14.2 and 12.3 eV, respectively).

A similar correlation to the metal−oxygen bond energy could not be made with respect to the deoxygenation affinity, which indicates that this reaction does not rely on the activation on oxygen vacancies in the support.

Taking the yield of cyclohexane as the primary parameter for the ranking, the apparent order of activity for HDO of phenol with nickel on different supports can be summarized as:

$$Ni/ZrO_2 > Ni\text{-}V_2O_5/ZrO_2 > Ni\text{-}V_2O_5/SiO_2 > Ni/Al_2O_3 > Ni/SiO_2 \gg Ni/MgAl_2O_4 > Ni/CeO_2\text{-}ZrO_2 \approx Ni/CeO_2 \gg Ni/C$$

It may be expected that the nickel crystallite particle size will influence the kinetics of the reactions, so it is important to note that the ranking presented here was made for catalysts with roughly the same nickel crystallite size (cf. Table 5).

Comparing k_2' values for Ni/ZrO_2, $Ni\text{-}V_2O_5/ZrO_2$, $Ni\text{-}V_2O_5/SiO_2$, Ni/Al_2O_3, and Ni/SiO_2 shows that all the values are on the same order of magnitude (ranging from 100 to 361 mL kg_{cat}^{-1} min^{-1}). The differences are probably related to support−metal interaction. However, $Ni/MgAl_2O_4$, Ni/CeO_2-ZrO_2, and Ni/CeO_2 all have lower k_2' values. For the $Ni/MgAl_2O_4$ catalyst, TPR showed that it was hard to reduce (cf. Table 4), indicating that part of the nickel is interacting with the support, which could be the reason for the poor performance of this catalyst. For the catalysts with Ce-containing supports, the carbon balance indicated a tendency toward cracking/coke formation, and therefore, the poor deoxygenation performance of these catalysts could be related to potential deactivation of the deoxygenating sites. No further investigations into these issues have been performed.

Obviously, Ni/C exhibited behavior markedly different from that of the other supports. Hence, this catalyst was tested in an experiment in which 50 g of cyclohexanol was used as feed with 1 g of catalyst at 100 bar and 275 °C for 4 h. In this experiment, a conversion of 47% was observed with a yield of 42% cyclohexane, the remaining product being primarily dicyclohexyl ether (4% yield). Thus, despite not being active for hydrogenation of the phenol ring, this catalyst was found to be active for deoxygenation. Calculating the kinetic constant for this reaction (corresponding to k_2') further showed that the deoxygenation capability of this catalyst was on the same order of magnitude as those of the other nickel catalysts, as shown in Table 5.

Hence, all catalysts supported on oxides are active for both hydrogenation and deoxygenation, but with different rates. In contrast, the carbon-supported catalyst is active for only the deoxygenation reaction. In a continuation of the discussion in the Introduction, it follows that the dual action of the catalyst primarily is required in the hydrogenation of complex molecules as phenol. On the other hand, the deoxygenation can take place on the nickel surfaces. Thus, we suggest a mechanism as sketched in Figure 8 for the HDO of phenol over nickel catalysts. The coordinatively unsaturated metal sites in the oxide surface often behave like Lewis acids, and the surface oxygen behaves like Lewis bases.[51] Thus, the activation of phenol on the oxide can take place through heterolytic dissociation of the O−H bond on the oxide where the hydrogen from the phenol is adsorbed on an oxygen site in the oxide surface layer and a metal vacancy site stabilizes the phenoxide ion. Generally, alcohols have been found to almost always adsorb through heterolytic dissociation on metal

dx.doi.org/10.1021/cs400266e | ACS Catal. 2013, 3, 1774−1785

oxides.[51] Supporting this, Popov et al.[54] observed phenoxide formation on Al_2O_3 when studying adsorption of phenol via IR spectroscopy. Liu et al.[55] concluded that when phenol is adsorbed at a Lewis acid site, one of the carbons in the aromatic ring becomes highly nucleophilic and thereby receptive to electrophiles, such as H^+. Thus, the phenoxide will interact with a nickel crystallite where hydrogen has been adsorbed, thereby facilitating the saturation of the double bounds and producing cyclohexanone. These steps are all illustrated in Figure 8. The cooperative effect of the support and active metal has also been found for the phenol hydrogenation on palladium catalysts where the activity for hydrogenation can be significantly increased by the introduction of a Lewis acid because of the activation of the phenol on the Lewis sites.[55−57]

The formed cyclohexanol can directly react with the exposed metallic nickel surfaces as shown in Figure 8 through adsorption at the OH group. The actual deoxygenation step probably takes place through a dehydration reaction, forming cyclohexene, as proposed in the reaction scheme of Figure 3. The cyclohexene can subsequently be hydrogenated into cyclohexane as the final product. This reaction mechanism is more complex than that discussed in the Introduction and Figure 1b.

In summary, among all tested catalysts, only those catalysts that showed both good hydrogenation and deoxygenation capabilities performed well, as a key step in the HDO of phenol under the tested conditions is the weakening of the C−O bond obtained by hydrogenation of the aromatic ring, as described in section 3. Hydrogenation of an aromatic hydrocarbon is, however, not trivial as these are considered to bind weakly to metal catalysts compared to conventional alkenes,[58,59] but adsorption on Lewis acid sites on the support appears to aid in this task.

5. CONCLUSIONS

Screening experiments have been performed to identify efficient catalysts for HDO of phenol at intermediate temperature and pressure (275 °C and 100 bar) in a batch reactor. Four groups of catalysts were investigated: oxide catalysts, methanol synthesis catalysts, reduced noble metal catalysts, and reduced non-noble metal catalysts, totaling 23 catalytic systems.

Across the series of investigated catalysts distinct differences were observed in the catalytic activity. Listing the apparent order of activity for all the tested catalysts, the following is found:

$$\begin{aligned}&Ni/ZrO_2 > Ni\text{-}V_2O_5/ZrO_2 > Ni\text{-}V_2O_5/SiO_2 > Ru/C\\ &> Ni/Al_2O_3 > Ni/SiO_2 \gg Pd/C > Ni/MgAl_2O_4\\ &> Ni/CeO_2\text{-}ZrO_2 \approx Ni/CeO_2 > Pt/C\\ &\gg Cu/ZnO/Al_2O_3 \approx NiO\text{-}MoO_3/Al_2O_3 \approx NiCu/SiO_2\\ &> Cu/SiO_2 > Co/SiO_2 > Ni/C > Fe/SiO_2, MnO/C\\ &, WO_3/C, V_2O_5/C, CoO\text{-}MoO_3/Al_2O_3\end{aligned}$$

The tested oxide and methanol synthesis catalysts had a low activity for the HDO of phenol under the given conditions, which was linked to their inability to hydrogenate the phenol ring. Reduced metal catalysts of both noble and non-noble metals were significantly more active. On these catalysts, HDO of phenol proceeds through an initial hydrogenation to cyclohexanone, which is rapidly hydrogenated to cyclohexanol. This can then in a second step be dehydrated to cyclohexene, which is rapidly hydrogenated to cyclohexane. The hydrogenation of the aromatic ring causes a weakening of the C−O bond, making the deoxygenation more favorable from cyclohexanol than from phenol.

A kinetic model revealed that the best hydrogenation catalyst not necessarily was the best deoxygenation catalyst. Pt/C, Ni/CeO_2, and Ni/CeO_2-ZrO_2 were found to be the best performing hydrogenation catalysts, with their effectiveness decreasing in that order, but were all found to have low activity for deoxygenation.

Nickel was the best performing reduced non-noble metal catalyst and was therefore tested on different supports. Oxide supports showed good activity, while a non-oxide support (as carbon) showed no activity for phenol HDO. However, Ni/C was active for HDO of cyclohexanol, showing that the activation of the phenol prior to the hydrogenation takes place on an oxygen vacancy site on the oxidic support, but the subsequent deoxygenation likely takes place directly on the nickel crystallites.

Noble metal catalysts, in contrast to nickel, performed well on carbon supports, showing that these metals on their own have the required affinity for phenol activation probably by direct interaction with the aromatic ring. Ruthenium was found to be the most active catalyst of the carbon-supported transition metals, but overall, Ni/ZrO_2 was the best performing catalyst, with balanced rates of both hydrogenation and deoxygenation. Thus, nickel appears to be a promising, less expensive catalyst for HDO.

■ ASSOCIATED CONTENT

Supporting Information

Derivation of the kinetic model, explanations of the assumptions made, and a final validation of the model. This material is available free of charge via the Internet at http://pubs.acs.org.

■ AUTHOR INFORMATION

Corresponding Author

*E-mail: aj@kt.dtu.dk.

Notes

The authors declare no competing financial interest.

■ ACKNOWLEDGMENTS

This work is part of the Combustion and Harmful Emission Control (CHEC) research center at The Department of Chemical and Biochemical Engineering at the Technical University of Denmark (DTU). This work is financed by DTU and The Catalysis for Sustainable Energy initiative (CASE), funded by the Danish Ministry of Science, Technology and Innovation. Flash calculations were conducted with SPECS version 5.62, which was kindly supplied by the Center for Energy Resources Engineering (CERE) at The Department of Chemical and Biochemical Engineering of DTU. We finally thank Bodil Fliis Holten (Center for Catalysis and Sustainable Chemistry, Department of Chemistry, DTU) for assistance with the measurements of the acidity of the catalysts.

REFERENCES

(1) Mortensen, P. M.; Grunwaldt, J.-D.; Jensen, P. A.; Knudsen, K. G.; Jensen, A. D. *Appl. Catal., A* **2011**, *407*, 1−19.
(2) Bridgwater, A. V.; Czernik, S.; Diebold, J.; Meier, D.; Oasmaa, A.; Peakocke, C.; Piskorz, J.; Radlein, D. *Fast Pyrolysis of Biomass: A Handbook*; CPL Press: Newbury, U.K., 1999.
(3) Holmgren, J.; Marinageli, R.; Nair, P.; Elliott, D. C.; Bain, R. *Hydrocarbon Process.* **2008**, 95−103.
(4) Raffelt, K.; Henrich, E.; Koegel, A.; Stahl, R.; Steinhardt, J.; Weirich, F. *Appl. Biochem. Biotechnol.* **2006**, *129*, 153−164.
(5) Zhang, W.; Zhan, Y.; Zhao, L.; Wei, W. *Energy Fuels* **2010**, *24*, 2052−2059.
(6) Garca, I.; Lopes, J. M.; Cerqueira, H. S.; Ribeiro, M. F. *Ind. Eng. Chem. Res.* **2013**, *52*, 275−287.
(7) Furimsky, E.; Massoth, F. E. *Catal. Today* **1999**, *52*, 381−495.
(8) Furimsky, E. *Appl. Catal., A* **2000**, *199*, 144−190.
(9) Moraes, M. S. A.; Migliorini, M. V.; Damasceno, F. C.; Georges, F.; Almeida, S.; Zini, C. A.; Jacques, R. A.; Caramão, E. B. *J. Anal. Appl. Pyrolysis* **2012**, *98*, 51−64.
(10) Moberg, D. R.; Thibodeau, T. J.; Amar, F. G.; Frederick, B. G. *J. Phys. Chem. C* **2010**, *114*, 13782−13795.
(11) Yakovlev, V. A.; Khromova, S. A.; Sherstyuk, O. V.; Dundich, V. O.; Ermakov, D. Y.; Novopashina, V. M.; Lebedev, M. Y.; Bulavchenko, O.; Parmon, V. N. *Catal. Today* **2009**, *144*, 362−366.
(12) Vargas, A.; Bürgi, T.; Baiker, A. *J. Catal.* **2004**, *222*, 439−449.
(13) Chorkendorff, I.; Niemantsverdriet, J. W. *Concepts of Modern Catalysis and Kinetics*; John Wiley & Sons, Inc.: New York, 2007.
(14) Chinchen, G. C.; Denny, P. J.; Parker, D. G.; Spencer, M. S.; Waugh, K. C.; Whan, D. A. *Appl. Catal.* **1987**, *30*, 333−338.
(15) Rasmussen, P. B.; Holmblad, P. M.; Askgaard, T.; Ovesen, C. V.; Stoltze, P.; Nørskov, J. K.; Chorkendorff, I. *Catal. Lett.* **1994**, *26*, 373−381.
(16) Askgaard, T.; Nørskov, J. K.; Ovesen, C. V.; Stoltze, P. J. *Catalysis* **1995**, *156*, 229−242.
(17) Vargas, A.; Reimann, S.; Diezi, S.; Mallat, T.; Baiker, A. *J. Mol. Catal.* **2008**, *282*, 1−8.
(18) Stakheev, A. Y.; Kustov, L. M. *Appl. Catal., A* **1999**, *188*, 3−35.
(19) Baltes, C.; Vukojevic, S.; Schüth, F. *J. Catal.* **2008**, *258*, 334−344.
(20) de Miguel Mercader, F.; Koehorst, P. J. J.; Heeres, H. J.; Kersten, S. R. A.; Hogendoorn, J. A. *AIChE J.* **2011**, *57*, 3160−3170.
(21) Schofield, K. *Prog. Energy Combust. Sci.* **2008**, *34*, 330−350.
(22) Llewellyn, P. L.; Bloch, E.; Bourelly, S. Surface Area/Porosity, Adsorption, Diffusion. In *Characterization of Solid Material and Heterogenous Catalysts*; Che, M., Védrine, J. C., Eds.; Wiley-VCH: Weinheim, Germany, 2012; Chapter 19, pp 853−880.
(23) Behrens, M.; Schlögl, R. X-ray Diffraction and Small Angle X-ray Scattering. In *Characterization of Solid Material and Heterogenous Catalysts*; Che, M., Védrine, J. C., Eds.; Wiley-VCH: Weinheim, Germany, 2012; Chapter 15, pp 611−654.
(24) Shuikin, N.; Erivanskaya, L. *Russ. Chem. Rev.* **1960**, *29*, 309−320.
(25) Zhao, C.; Kuo, Y.; Lemonidou, A. A.; Li, X.; Lercher, J. A. *Angew. Chem., Int. Ed.* **2009**, *48*, 3987−3990.
(26) Zhao, C.; He, J.; Lemonidou, A. A.; Li, X.; Lercher, J. A. *J. Catal.* **2011**, *280*, 8−16.
(27) Ohta, H.; Kobayashi, H.; Hara, K.; Fukuoka, A. *Chem. Commun.* **2011**, *47*, 12209−12211.
(28) Zhao, C.; Kasakov, S.; He, J.; Lercher, J. A. *J. Catal.* **2012**, *296*, 12−23.
(29) Ryymin, E.-M.; Honkela, M. L.; Viljava, T.-R.; Krause, A. O. I. *Appl. Catal., A* **2010**, *389*, 114−121.
(30) Venderbosch, R. H.; Ardiyanti, A. R.; Wildschut, J.; Oasmaa, A.; Heeres, H. J. *J. Chem. Technol. Biotechnol.* **2010**, *85*, 674−686.
(31) Benson, S. W. *Thermochemical Kinetics: Methods for estimation of thermochemical data and rate parameters*; John Wiley & Sons, Inc.: New York, 1968.
(32) Fogler, H. S. *Elements of Chemical Reaction Engineering*; Prentice Hall: Upper Saddle River, NJ, 2006.
(33) Prasomsri, T.; Nimmanwudipong, T.; Román-Leshkov, Y. *Energy Environ. Sci.* **2013**, *6*, 1732−1738.
(34) Adriyanti, A. R.; Khromova, S. A.; Venderbosch, R. H.; Yakovlev, V. A.; Heeres, H. J. *Appl. Catal., B* **2012**, *117*−*118*, 105−117.
(35) Elliott, D. C.; Hart, T. R. *Energy Fuels* **2009**, *23*, 631−637.
(36) Davda, R. R.; Shabaker, J. W.; Huber, G. W.; Cortright, R. D.; Dumesic, J. A. *Appl. Catal., B* **2005**, *56*, 171−186.
(37) Wildschut, J.; Mahfud, F. H.; Venderbosch, R. H.; Heeres, H. J. *Ind. Eng. Chem. Res.* **2009**, *48*, 10324−10334.
(38) Lee, C. R.; Yoon, J. S.; Suh, Y.-W.; Choi, J.-W.; Ha, J.-M.; Suh, D. J.; Park, Y.-K. *Catal. Commun.* **2012**, *17*, 54−58.
(39) Adriyanti, A. R.; Gutierrez, A.; Honkela, M. L.; Krause, A. O. I.; Heeres, H. J. *Appl. Catal., A* **2011**, *407*, 56−66.
(40) Nørskov, J. K.; Rossmeisl, J.; Logadottir, A.; Lindqvist, L.; Kitchin, J. R.; Bligaard, T.; Jonsson, H. *J. Phys. Chem. B* **2004**, *108*, 17886−17892.
(41) Foster, A. J.; Do, P. T. M.; Lobo, R. F. *Top. Catal.* **2012**, *55*, 118−128.
(42) Zielinski, J. *J. Chem. Soc., Faraday Trans.* **1997**, *93*, 3577−3580.
(43) Dry, M. E. *J. Chem. Technol. Biotechnol.* **2001**, *77*, 43−50.
(44) Dry, M. E. *Catal. Today* **2002**, *71*, 227−241.
(45) Dry, M. E. FT Catalysts. In *Fischer−Tropsch Technology*; Steynberg, A., Dry, M., Eds.; Elsevier: Amsterdam, 2004; Chapter 7, pp 533−593.
(46) Rostrup-Nielsen, J. R. Steam Reforming. *Handbook of Heterogeneous Catalysis*; John Wiley & Sons, Inc.: New York, 2008; Chapter 13.11, pp 2882−2905.
(47) Filley, J.; Roth, C. *J. Mol. Catal.* **1999**, *139*, 245−252.
(48) Burwell, R. L.; Littlewood, A. B.; Cardew, M.; Pass, G.; Stodhart, C. T. H. *J. Am. Chem. Soc.* **1960**, *82*, 6272−6280.
(49) Burwell, R. L.; Taylor, K. C.; Haller, G. L. *J. Phys. Chem.* **1967**, *71*, 4580−4581.
(50) Rodriguez, J. A.; Hanson, J. C.; Frenkel, A. I.; Kim, J. Y.; Perez, M. *J. Am. Chem. Soc.* **2002**, *124*, 346−354.
(51) Kung, H. H. Surface Coordinative Unsaturation. *Transition Metal Oxides: Surface Chemistry and Catalysis*; Elsevier: Amsterdam, 1989; Chapter 4, pp 53−71.
(52) Rethwisch, D. G.; Dumesic, J. A. *Langmuir* **1986**, *2*, 73−79.
(53) Idriss, H.; Barteau, M. A. *Adv. Catal.* **2000**, *45*, 261−331.
(54) Popov, A.; Kondratieva, E.; Gilson, J.-P.; Mariey, L.; Travert, A.; Mauge, F. *Catal. Today* **2011**, *172*, 132−135.
(55) Liu, H.; Jiang, T.; Han, B.; Liand, S.; Zhou, Y. *Science* **2009**, *326*, 1250−1252.
(56) Velu, S.; Kapoor, M. P.; Inagaki, S.; Suzuki, K. *Appl. Catal., A* **2003**, *245*, 317−331.
(57) Matos, J.; Corma, A. *Appl. Catal., A* **2011**, *404*, 103−112.
(58) Boitiaux, J. P.; Cosyns, J.; Robert, E. *Appl. Catal.* **1987**, *32*, 145−168.
(59) Ponec, P.; Bond, G. C. Catalytic hydrogenation and dehydrogenation. *Catalysis by Metals and Alloys*; Elsevier: Amsterdam, 1995; Vol. *95*, Chapter 11, pp 477−539.